European Review for Medical and Pharmacological Sciences 2020; 24: 3331-3343

Calcium-calmodulin-dependent protein kinase type 2 induces apoptosis of hepatocytes after liver transplantation

W. LI, X.-B. ZHANG, R.-C. WU, S.-N. ZHANG, J. LIU, Y. GAO, K.-P. ZHENG, J.-H. RAN

Department of Hepatobiliary Pancreas and Vascular, Ganmei Hospital Affiliated to Kunming Medical University, Kunming, Yunnan, China

Abstract. – OBJECTIVE: The warm ischemia-reperfusion injury confines the prevalence of allografts. To improve the success rate of allotransplantation, we designed experiments to study the mechanism of calcium-calmodulin-dependent protein kinase type 2 (CaMK II) in ischemia-reperfusion (I/R) injury.

MATERIALS AND METHODS: We established the I/R model in SD rats and performed the liver transplantation (LT). As a result, the expression of CaMK II in tissues was detected. CaMK II was interfered with and overexpressed by the transference of the lentivirus vector, and the hepatocyte apoptosis and viability were inspected. At the same time, the content of cytochrome c and apoptosis-inducing factor (AIF) were determined. The measurement of mitochondrial membrane potential and detection of intercellular calcium levels were performed.

RESULTS: The expression of CaMK II significantly increased and is highly corresponded with the duration of warm ischemia. In BRL-3A cells and liver tissues, increased cellular apoptosis and less viability had been observed in the CaMK II overexpression group. Cytochrome c and AIF were also largely increased compared to the interfered group. Moreover, apparent mitochondrial membrane potential loss has also been detected in the CaMK II overexpression group.

CONCLUSIONS: It suggested that CaMK II induces cell apoptosis. Our findings may give a novel indication that inhibition of CaMK II could be a new way for the therapy of warm ischemia-reperfusion injury after LT in future clinical practice.

Key Words:
Calcium-calmodulin-dependent protein kinase type 2, Ischemia-reperfusion injury, Liver transplantation, Apoptosis.

Abbreviations

I/R injury, ischemia reperfusion injury; LT, liver transplantation; CaMK II, calcium-calmodulin-dependent protein kinase type 2; AIF, apoptosis inducing factor; TUNEL, TdT-mediated dUTP nick end labeling; WIT, warm ischemia time; DCD, donation after circulatory death; Min, minute(s); H, hour(s); IHC, immunohistochemical; WB, Western blot; qRT-PCR, quantitative reverse transcription polymerase chains reaction; TUNEL, terminal-deoxynucleoitidyl transferase mediated nick end labeling; H&E, hematoxylin-eosin; rpm, evolution per minute; FCCP, carbonyl cyanide 4-(trifluoromethoxy) phenylhydrazone; LV, lentivirus; NC, negative control; Sh, short hairpin RNA; ALT, alanine aminotransferase; AST, aspertate aminotransferase; SD rat sprague dawley rats; PBS, phosphate-buffered saline; ER, endoplasmic reticulum; ROS, reactive oxygen species; RIPA, radioimmunoprecipitation assay; TBST, Tris-Buffered Saline and Tween-20; DMEM, Dulbecco's Modified Eagle's Medium; PI, propidium iodide; BSA, bovine serum albumin; D, day(s); GEO, gene expression omnibus; PVDF, polyvinylidene difluoride; DMSO, dimethyl sulfoxide.

Introduction

Worldwide, donor liver donations after circulatory death (DCD) has been endorsed for decades, and it has become an increasing source of allografts[1-4]. As reported, liver from DCD occupied about 30% of all liver transplants[5]. However, the use of DCD liver for transplantation in clinicals remains cautious due to the WIT, which is the most important risk factor affecting tissue viability and graft function[6,7]. The DCD donors often suffer from trauma, hemorrhagic shock or cardiac arrest, this low-flow perfusion status is known as warm ischemia[8]. During the warm ischemia, livers from DCD donors inevitably go through hypotension, hypoxia, and ischemia/reperfusion injury[9,10]. Under this condition, liver after transplant may undergo varying degrees of damages with the prolonged warm ischemia, and the liver is more liable to suffer from primary graft dysfunction and biliary complications[11-13]. Therefore, a method to recover the function of the liver that

Corresponding Author: Jiang-Hua Ran, MD; e-mail: rjh2u@163.com

suffers from warm ischemia reperfusion injury is the foundation to which DCD can be used in clinical trials.

Current research has proven that I/R injury is able to cause transition in mitochondrial membrane potential ($\Delta\psi m$)[14,15]. Furthermore, when the mitochondrial permeability transition pore opens, Ca^{2+} overloading leads to mitochondria swelling, and mitochondrial integrity is impaired and proapoptotic factors are release into the cytoplasm[16,17]. Ultimately, these pathological changes accelerated cell death. Therefore, mitochondrial dysfunction is closed related to the I/R injury, and the target to timely maintain the mitochondria stability can protect the tissue survival from post-transplantation[8].

CaMK II is a serine/threonine protein kinase and it is capable of acquiring the increasing intracellular Ca^{2+}. When combined with Ca^{2+}/CaM-binding, CaMK II undergoes activation by autophosphorylation; activating CaMK II can phosphorylate certain enzymes and regulates cell activity[18,19]. The activation of CaMK II has a hand in the regulation of cell apoptosis[20-22]. Joiner et al[23], it also has been verified that the expression of CaMK II promotes the apoptosis of myocardial cell after suffering from warm ischemia reperfusion injury. However, the mechanism of CaMK II regulation of post-liver transplantation is not clear.

In this paper, we reported the role of CaMK II in the liver, which was used in transplantation. Our data revealed overexpression of CaMK II could induce hepatocytes apoptosis. It will provide a candidate target for the treatment of ischemia-reperfusion injury in future clinic trials.

Materials and Methods

Animal Care

Sprague Dawley (SD) rats (Seven-week old, 250-300 g) were bought from Experimental Animal Center of Kunming Medical University. They were placed in a pathogen-free room. The animal study protocol is legally approved by the Animal Care & Welfare Committee of Kunming Medical University. The approval number is: 2019-04. Experiments complied with the Guide that the Care and Use of Laboratory Animal published by the US National Institutes Health and the provisions of the Declaration of Helsinki. Experiments were performed under anesthesia that minimizes the pain of the animals.

Establishment of I/R Injury Model and Tissue Harvest

To determine if the expression of CaMK II is related to the WIT, we constructed the I/R injury model of SD rats. The rats were anesthetized with isoflurane using cone masks (2% during the operation, 1 l/ml airflow, a fraction of inspiration O_2 70%). A median and transverse laparotomy was performed in the supine position to expose the heart. 10 μl of heparin was dissolve in 1 ml of normal saline and injected into the rats through the dorsal vein of the penis. Finally, the thoracic aorta and superior vena cava were occluded with a traumatic vascular clamp to mimic the process of heart arrest for 0, 10 and 20 minutes (min). After the duration, 20 ml of cold Ringer's lactate (Tuopai pharmaceutical Co., Ltd. Sichuan, China) was gently flushed into the livers. The livers were then isolated from the rats. The collected organs were stored in −80°C for further use. The transplantation operation was performed as previously described[24].

Immunohistochemical (IHC) Staining

To detect the expression of CaMK II protein in liver tissue, the liver tissue samples which had been sliced and dewaxed were used for immunohistochemical analysis. The sections were heated to repair the antigen, and hatched at room temperature with the peroxidase blocking reagent for 10 min followed by washing with PBS (Hyclone, South Logan, UT, USA) for 3 × 3 min. The sections were then hatched with CaMKII antibody (Merck Millipore, Darmstadt, Germany) for 12 h at 4°C and rinsed with PBS (Hyclone, South Logan, UT, USA) for 3 × 3 min. Afterwards, the sections were cultivated with the secondary antibody (Proteintech, Rosemont, IL, USA) at normal temperature for 30 min. After repeating the process of washing with PBS (Hyclone, South Logan, UT, USA) 3 times, the sections were hatched using 3, 3'-diaminobenzidine (MaixinBiotechnique, Fuzhou, China) for 5 min. These sections were then washed with tap water and double steamed water for 10 min and 5 min respectively, and counterstained with hematoxylin for 20 seconds. The sections were rinsed with hydrochloric acid alcohol for 5 min and flushed to return to blue. It was then dehydrated using gradient alcohol, cleared with xylene and mounted with neutral gum. In 24 hours (h), the sections were observed and photographed using an optical microscope.

Western Blot (WB)

To detect the level of CAMK II, AIF and cytochrome *c* in BRL-3A cells and liver tissues, we preformed WB. Firstly, the BRL-3A cells and liver tissues were dealt with lysis/RIPA (Beyotime Biotechnology, Shanghai, China) buffer which containing 1% proteinase inhibitor for 5 min. Then, homogenates were centrifuged at 16000 rpm for 10 min at 4°C and purity of protein were measured by an assay kit (Bio-Rad, Hercules, CA, USA). After that, the acquisitions were isolated by gel electrophoresis and transferred to PVDF membranes, the membranes were blocked for 2 h in bovine serum albumin/TBST buffer (Becton Dickinson, Franklin Lakes, NJ, USA, 5% dried skimmed milk). Next, membranes were incubated with antibodies of CaMK II, AIF, and cytochrome *c* (Cell Signaling Technology, Inc., Danvers, MA, USA) for 12 h at 4°C, β-actin was adopted to an internal control. The membranes were washed thrice with TBST before reacting with secondary antibody (Protein Technology, Chicago, IL, USA) for 2 h at room temperature. Finally, the proteins were visualized scanned in LumiGlo substrate (Super Signal West Pico Trial Kit, Pierce, USA) with enhanced chemiluminescence (ECL).

Quantitative Reverse Transcription Polymerase Chain Reaction (qRT-PCR)

The expression of CAMK II mRNA was detected by the qRT-PCR method. As the first step, total RNA was extracted by TRIzol agentia (Invitrogen Corp, Carlsbad, CA, USA), and its consistence and purity were determined. Then, the synthesis of cDNA is on the basis of reverse transcription kit (TaKaRa Biotechnology Co., Ltd., Komatsu, Japan). All primers for qRT-PCR were produced by Sangon (Sangon Biotech Co., Ltd., Shanghai, China), the sequences were showed in Table I. PCR was performed using a thermocycler: 95°C for 3 min, 95°C for 15 s, 60°C for 1 min, the total for 40 cycles. The data was analyzed by the comparative critical threshold (Ct) method, and the relative expression was analyzed by normalization to β-actin values using the $2^{-\Delta\Delta}$Ct method.

Table I. The primer sequences of qRT-PCR.

rat-CaMK II-S	5'-ACACAGGAATATGCTGCAAAAAT-3'
rat-CaMK II-A	5'-GGAGCACAAACTGGAACAATGAC-3'
rat-β-actin-S	5'-TGGGTATGGAATCCTGTGGCA-3'
rat-β-actin-A	5'-GGCATTTCTGGAGATACGGTTGT-3'

S: sense; A: anti-sense.

GEO2R Analysis

For further verification of the CaMK II expressed in the human liver tissues after LT, we screened the microarray data and corresponding clinical data of LT from the public Gene Expression Omnibus (GEO) database: GEO accession number GSE14951. For this dataset, gene expression in livers from DCD undergoing 50 ± 10 min of WIT was compared to the liver from the normal patient. GEO2R (www.ncbi.nlm.nil.gov/geo/geo2r) was used to analyze the microarray data.

Cell Culture

The rat hepatic cell lines BRL-3A were all bought from the Chinese Academy of Sciences (Kunming, China) and melted in a water bath at 37ºC. After 2 min, the cell suspension was taken out and diluted at 1:4 (1 ml cell suspension, 4 mL medium) into the centrifuge tube at 1000 rpm for 3 min at room temperature. Then, cells were resuspended by 2 ml medium. Next, the cells were sucked up and put into a culture flask containing 10 ml medium, the culture bottle was bred in the thermotank at 37°C and containing 5% CO_2. Finally, BRL-3A were raised in DMEM (Gibco, Grand Island, NY, USA).

CaMK II Overexpression and Downregulation

Lentivirus carrying scramble or LV-CaMK II or LV-sh-CaMK II construct was bought from Shanghai Genechem Co., Ltd. The following sequences were used: forward: 5'-GCGGTAGGCGTGTACGGT-3'and reverse: 5'-ATTGTGGATGAATACTGCC-3' for LV-CaMK II; forward: 5'-TAATACGACTCACTATAGGG-3' and reverse: 5'-CTGGAATAGCTCAGAGGC-3' for LV-sh-CaMK II.

In vitro, BRL-3A cells were incubated in a 6-well plates and cultured in an incubator (5% CO_2) at 37ºC. When the cell convergence rate was between 50% and 70%, lentivirus was added and cultured for 12 h. *In vivo*, lentivirus was transfected into the liver by tail vein injection.

Annexin V/Propidium Iodide Staining Assay

Cells were incubated with 1×10^7 copies of LV-sh-CaMK II, LV-CaMK II, LV-sh-CaMK II-NC or LV-CaMK II-NC for 1 d. Cells apoptosis were identified byz Annexin V-FITC and propidium iodide (Becton Dickinson, Franklin Lakes, NJ, USA) dual staining. Briefly, cells were transferred to centrifuge tube and 1×10^5 cells were collected.

Then, cells were centrifuged at 2000 rmp for 5 min and re-suspended in 500 μL of 1× binding buffer. Next, 5 μL of Annexin V-FITC was dropped in the cells and cells were hatched for 0.5 h at 4°C in the dark. Later, cells were incubated with 10 μL of propidium iodide for another 5 min. Apoptotic cells were then immediately measured by flow cytometer (Becton Dickinson, Franklin Lakes, NJ, USA).

Cell Viability Assay

BRL-3A cells were paved at a density of 5 × 10^3 cells/well in 96-well plates for 24 h. After the adhesion, cells were transfected with 1×10^7 copies of LV-sh-CaMK II, LV-CaMK II, LV-sh-CaMK II-NC, and LV-CaMK II-NC. The cells were then cultured for another 1, 2, 3, 4, 5, and 6 days. Then, Cell Counting Kit-8 (CCK-8, Dojindo Molecular Technologies, Kumamoto, Japan) was drop in (10 μl/well), and the liquid was placed at 37°C for 30 min. Finally, the absorbance OD of the liquid was checked by a microplate reader at 450 nm.

Terminal-Deoxynucleoitidyl Transferase dUTPnick End Labeling (TUNEL) Staining

To detect apoptosis in liver tissue after LT, a one-step TUNEL Apoptosis Assay kit (Roche, Basel, Switzerland,) was used. Briefly, the 4 μm thick paraffin sections were dewaxed and air-dried. Then, proteinase K was mixed and treated for 20 min. After that, it was incubated in a mixture of the fluorescent labeling solution of dUTP and the TdT enzyme at 37°C for 1 h. The sections in positive group were cultivated for 10 min with DNaseI at 25°C. The negative controls were bred with dUTP at room temperature for 10 min. The samples were then disposed with diaminobenzidine (DAB), counterstained with hematoxylin, dehydrated in a gradient series, vitrified with dimethyl benzene, and mounted with neutral balsam.

Hematoxylin-Eosin(H&E) Staining

H&E staining was adopted to watch the pathological changes of liver tissue after transplantation. The method is as follows: after the rats were euthanized, the liver tissue sections were dewaxed and dehydrated, and hematoxylin solution was added and stained at room temperature for 10 min. The hematoxylin was washed away with water. 1 ml of 0.5% eosin solution was dripped into the sections, dyed at normal temperature for 60 min, and washed with running water for several seconds. The sections were then dehydrated with graded alcohol and xylene. Neutral gum was used to seal the sections, and the pathological changes of liver tissue were observed by an optical microscope.

Liver Function Test

After LT, the blood samples collected from the orbit of rats. The contents of ALT and AST were analyzed by the automatic biochemical analyzer (Beckman AU5400, CA, USA).

Measurement of Mitochondrial Membrane Potential

Firstly, 1 ml of 1.0% protease XXIV in assay buffer was injected in fresh rat tissues. Tissues were homogenized and cells were harvested after centrifuged at 1000 rpm for 10 min. Then, cells were transferred to HTF culture media that append 0.5% BSA (Hyclone, South Logan, UT, USA) after washed with 2 ml of PBS (Hyclone, South Logan, UT, USA) and incubated in > 85% humidity (37°C, 20% O_2, 5% CO_2). The cells of positive group were incubated with FCCP (Carbonyl cyanide 4-(trifluoromethoxy) phenylhydrazone) for 20 min before adding the JC-10, and the cells of treatment groups was hatched with acrolein and CTX (25 μM) at incubator for 45 min. Then, the cells from all the groups were cultivated with HOEST dye at 37°C for 20 min (20% O_2, 5% CO_2). For further analysis, each group of cells was washed, dissolved in 0.25% trypsin, and resuspended in PBS. Fluorescence signal was detected by flow cytometry on an LSR II-12 (Becton Dickinson, Franklin Lakes, NJ, USA) in green (emission: 525 nm) and red (emission: 590 nm) channels.

Detection of Intercellular Calcium Level

Liver tissues were treated as stated in measurement of mitochondrial membrane potential. The lysis of Flou-3 AM probe (Sigma-Aldrich, St. Louis, MO, USA) was carried out in DMSO with a final concentration of 1 μM and added to the cell suspension. The sample was cultivated in incubator for 0.5 h. The sample obtained was well mixed and transferred into 10 equal microtubes, each tube contained 400 μl of the sample. To remove additional Flou-3 AM, all the microtubes were centrifuged for 5 min. The sediment was re-suspended to a volume of 500 ml using Ham's F10 (Gibco, Grand Island, NY USA). All experimental groups were transferred to the flow cytometry tube. The data were calculated using the FlowJo Software.

Statistical Analysis

The data in the experiment were expressed as the mean ± standard deviation of the three independent experiments and SPSS 19.0 was used for statistical analyses. Student's *t*-tests were used to compare the averages of the two groups, and Bonferroni's-corrected one-way ANOVA is used to compare the averages of three or more groups. *p<0.05 was indicated as a statistical significance.

Results

CaMK II Expression in the Liver Tissues Is Significantly Increased After LT

To determine the expression change of CaMK II in liver tissues after transplantation, we first constructed the I/R models with prolonged WIT. The WB, IHC staining, and qRT-PCR tests were also conducted. As a result, when the WIT was prolonged to 10 min and 20 min, CaMK II protein level was largely increased when compared with the normal group (Figure 1A and B, p<0.05). The CaMK II protein appeared strongly positive when the duration was 20 min as compared to the other two groups in D7 (Figure 1C). Up-regulated CaMK II mRNA expression was observed in D7 (Figure 1D, p<0.05). GEO2R analysis showed that the CaMK II expression was higher in DCD patients than the norm patients (Figure 1E, p<0.05), which was the same as our findings. The above observation indicated CaMK II expression level significantly increases after LT.

The Apoptosis of BRL-3A Cells Increased With the Increase of CaMK II, and Decreased With the Decrease of CaMK II

To analyze the effects of CaMK II on hepatocyte, we applied lentivirus carrying sh-RNA specifically targeting CaMK II, and lentivirus carrier overexpression of CaMK II carriers to transfer BRL-3A cells. Mock-vehicle groups and saline groups were designed as control groups. Western blot confirmed that LV-sh-CaMK II and LV-CaMK II succeeded in significantly knocking down and overexpressing CaMK II in cell lines (Figure 2A and B). Flow cytometry assay show that the apoptosis frequency of BRL-3A cells were increased in the LV-CaMK II group and decreased in LV-sh-CaMK II group compared with control group (Figure 2C, p<0.05). The S phase of BRL-3A cells were prolonged in LV-sh-CaMK II group and shortened in LV-CaMK II group when compared to the control group (Figure 2D). Simultaneously, the CCK8 assay detected the cell viability was increased after inhibiting the CaMK II (Figure 2E, p<0.05). CaMK II induction appears to reduce BRL-3A cells survival, and CaMK II inhibited increase BRL-3A cells proliferation.

Cytochrome c and AIF Increase With the Overexpression of CaMK II

To evaluate whether CaMK II augmented apoptosis through cytochrome *c* /AIF activation, we overexpressed and inhibited CaMK II in BRL-3A cells and detected the expression of cytochrome *c* and AIF by WB. Indeed, the overexpression of CaMK II enhanced the expression of cytochrome *c* and AIF. After interfering with the expression of CaMK II, the level of cytochrome *c* and AIF has declined accordingly (Figure 3A to D, p<0.05). It confirmed CaMK II can regulate the level of cytochrome *c* and AIF, and participates in the progress of hepatocyte apoptosis.

The High Level of CaMK II Is Accompanied by Increased Hepatocyte Apoptosis and Liver Function Injury In Vivo

The effects of CaMK II on liver transplantation *in vivo* were assessed using the liver transplantation models of SD rats with 10 min of WIT. Lentivirus with a CaMK II over-expressing sequence (LV-CaMK II) or sh-CaMK II (LV-sh-CaMK II) was transfected into the liver by tail intravenous injection. The rats' serum for detecting the level of ALT and AST were collected from the 1st, 3rd and 7th day after the operation. The rats were euthanized at D7, and the data was analyzed. As a result, the fluorescence microscope showed lentivirus with the carrier of LV-CaMK II and LV-sh-CaMK II was symmetrically distributed in the liver (Figure 4A). qRT-PCR analysis confirms that CaMK II was interfered with and over-expressed successfully in the liver tissue (Figure 4B, p<0.01). TUNEL staining showed that the liver tissues appeared to have more cell apoptosis in the LV-CaMK II group than the control group (p<0.05), and there is a lower apoptosis rate in LV-sh-CaMK II group (Figure 4C and D, p<0.01). The liver function test showed that the AST and ALT in serum were increased over time, and both AST and ALT were increased in the LV-CaMK II group at D7. On the contrary, the level of AST significantly declined at D7 in the LV-sh-CaMK II group compared to the control group (Figure 4E and F, p<0.01). The result of H&E staining indicates that there is an acidophilic change in 3 control groups, and spotty necrosis was found in the LV-CaMK II group. The LV-sh-CaMK II group represents the cell division phase (Figure 4G).

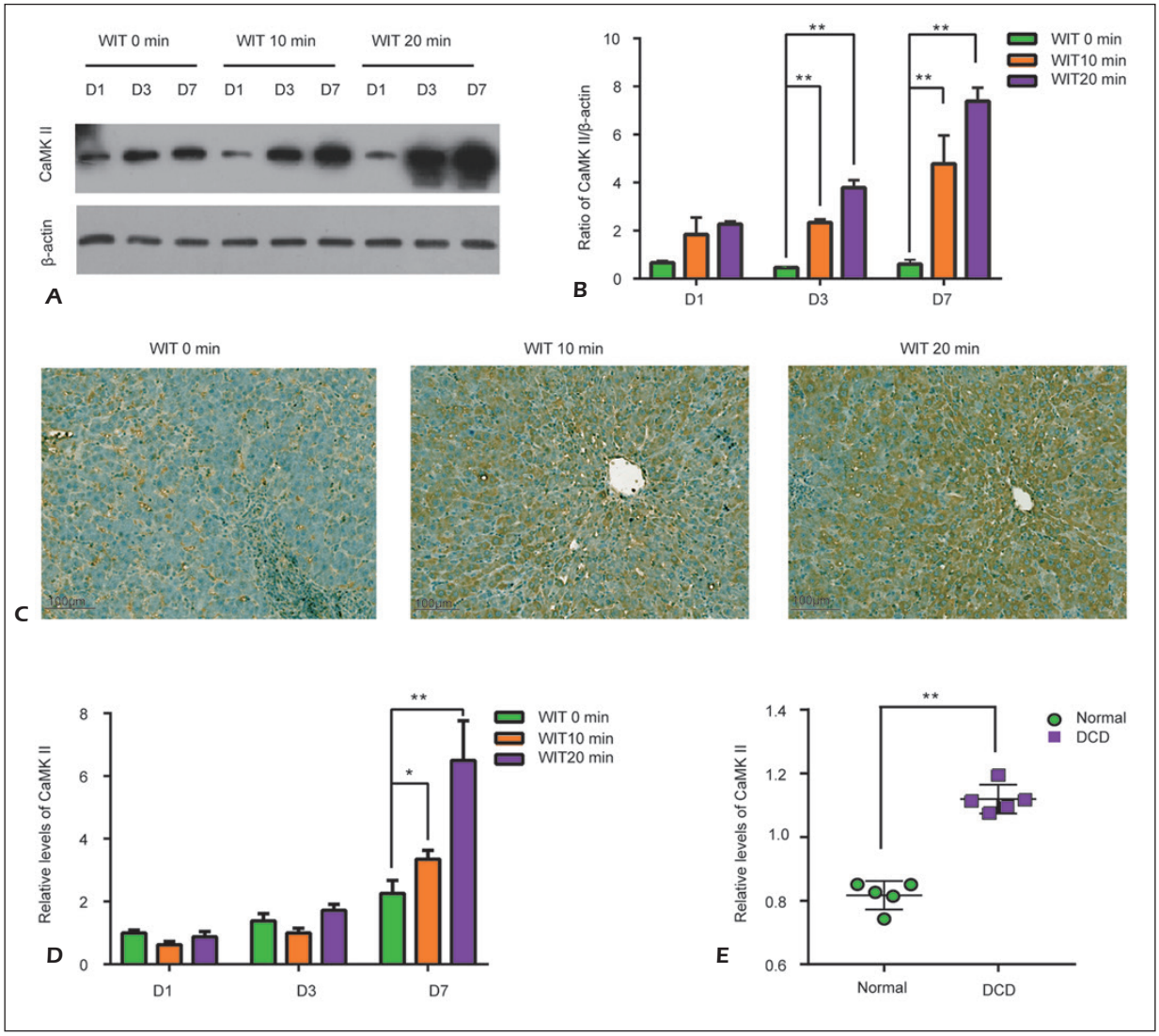

Figure 1. The expression of CaMK II in the liver after I/R injury. **A**, The protein bands of CaMK II in D1, D3, and D7 after the I/R injury with different WIT (0 min, 10 min, and 20 min). CaMK II: calcium-calmodulin-dependent protein kinase type 2; D: day; WIT: warm ischemia time; min: minute(s); (n = 6/group). **B**, The histogram of CaMK II protein in D1, D3 and D7 after the I/R injury with different WIT (0 min, 10 min, and 20 min). CaMK II: calcium-calmodulin-dependent protein kinase type 2; D: day; WIT: warm ischemia time; min: minute(s); (n = 6/group, $^{**}p<0.01$). **C**, The immunohistochemical of CaMK II in D1, D3, and D7 after the I/R injury with different WIT (0 min, 10 min, and 20 min). The brown dots represent marked CaMK II proteins. WIT: warm ischemia time; min: minute(s); (n = 6/group, scale bar = 100 μm). **D**, The relative expression of CaMK II mRNA in D1, D3, and D7 after the I/R injury with different WIT (0 min, 10 min, and 20 min). CaMK II: calcium-calmodulin-dependent protein kinase type 2; D: day; WIT: warm ischemia time; min: minute(s); (n = 6/group, $^{**}p<0.01$). **E**, The relative expression of CaMK II in normal liver cells and DCD liver cells. The green circles represent normal liver cells, and the purple boxes represent DCD liver cells. CaMK II: calcium-calmodulin-dependent protein kinase type 2; DCD: donation after circulatory death; (n = 8/group, scale bar = 50 μm, $^{*}p<0.05$, $^{**}p<0.01$).

These results illustrate that CaMK II is successfully overexpressed and suppressed in liver cells, and the up-regulated CaMK II induced the apoptosis of hepatocyte and liver function injury in SD rats. However, inhibition of CaMK II will induce the proliferation of hepatocytes and recovery of liver function.

The Up-Regulation of CaMK II Leads to Mitochondrial Dysfunction and Up-Regulation of Cytochrome c and AIF

For further study of the apoptotic pathway, we detected the level of cytochrome c and AIF, the change of mitochondrial morphology and membrane potential, and the concentration of Ca^{2+} in rat hepatocytes.

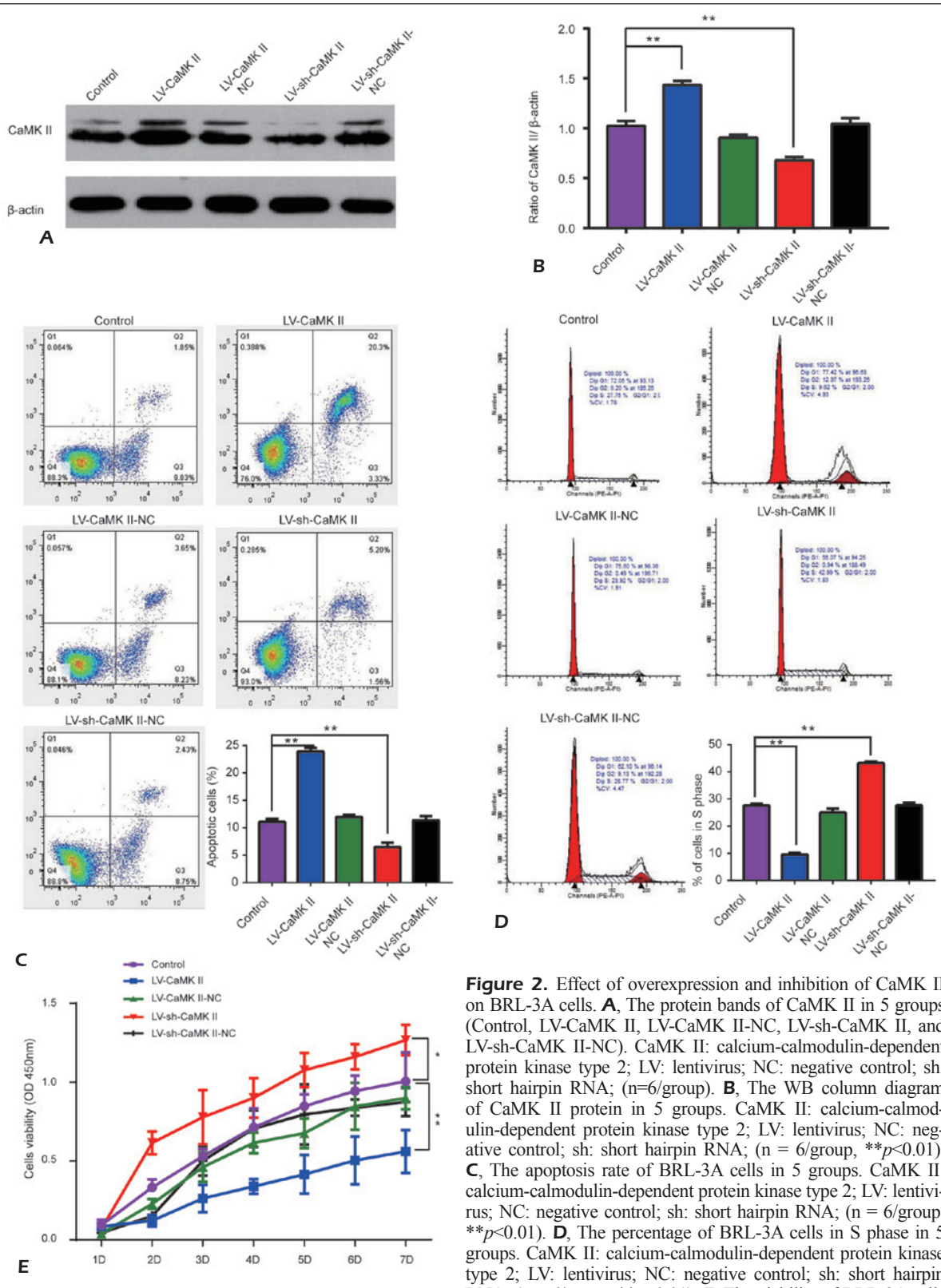

Figure 2. Effect of overexpression and inhibition of CaMK II on BRL-3A cells. **A**, The protein bands of CaMK II in 5 groups (Control, LV-CaMK II, LV-CaMK II-NC, LV-sh-CaMK II, and LV-sh-CaMK II-NC). CaMK II: calcium-calmodulin-dependent protein kinase type 2; LV: lentivirus; NC: negative control; sh: short hairpin RNA; (n=6/group). **B**, The WB column diagram of CaMK II protein in 5 groups. CaMK II: calcium-calmodulin-dependent protein kinase type 2; LV: lentivirus; NC: negative control; sh: short hairpin RNA; (n = 6/group, $^{**}p<0.01$). **C**, The apoptosis rate of BRL-3A cells in 5 groups. CaMK II: calcium-calmodulin-dependent protein kinase type 2; LV: lentivirus; NC: negative control; sh: short hairpin RNA; (n = 6/group, $^{**}p<0.01$). **D**, The percentage of BRL-3A cells in S phase in 5 groups. CaMK II: calcium-calmodulin-dependent protein kinase type 2; LV: lentivirus; NC: negative control; sh: short hairpin RNA; (n = 6/group, $^{**}p<0.01$). **E**, The viability of BRL-3A cells in 5 groups. CaMK II: calcium-calmodulin-dependent protein kinase type 2; LV: lentivirus; NC: negative control; sh: short hairpin RNA; (n = 6/group).

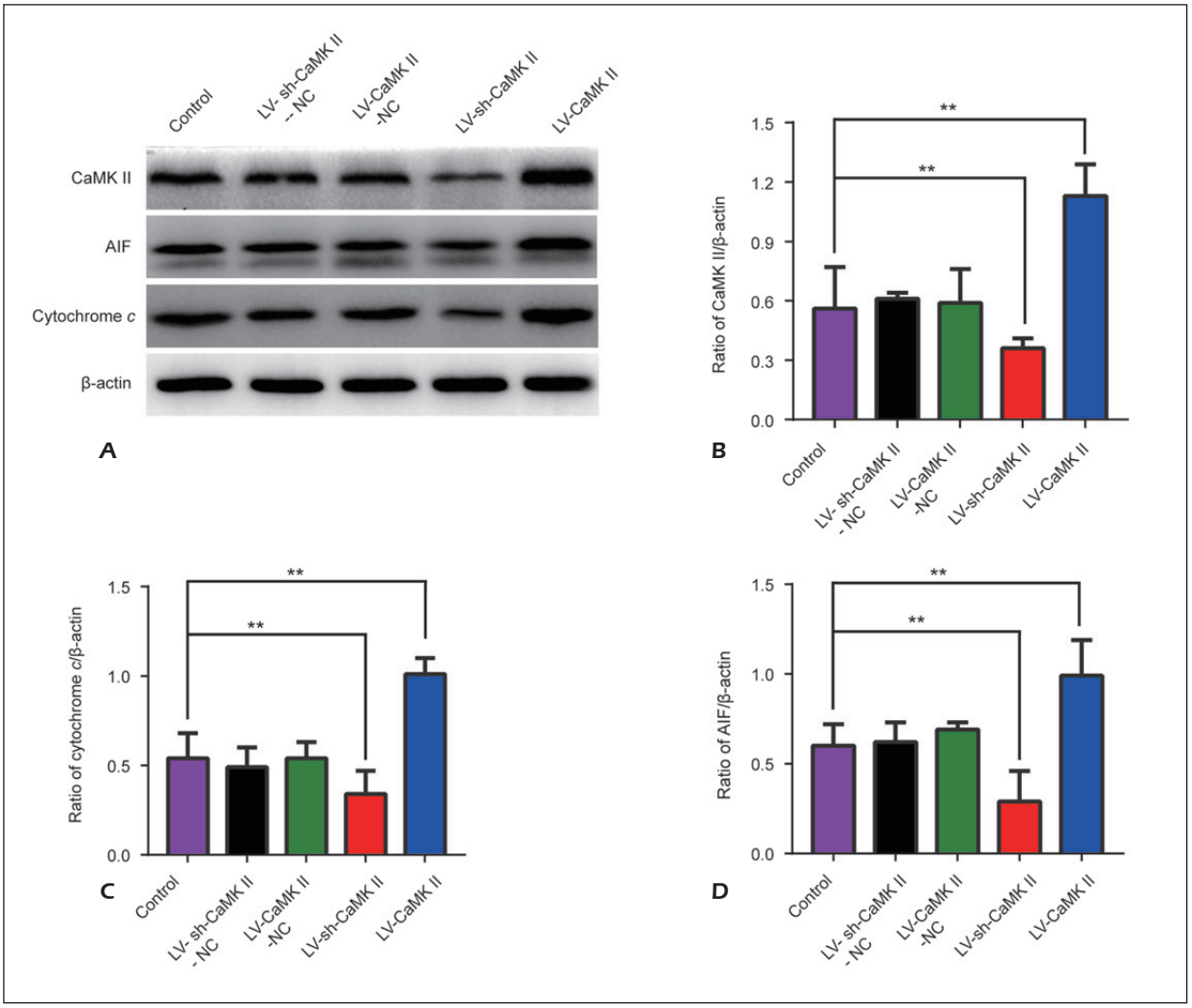

Figure 3. The expression of CaMK II, cytochrome c, and AIF in BRL-3A cells. **A**, The protein bands of CaMK II, cytochrome c, and AIF in 5 groups (Control, LV-CaMK II, LV-CaMK II-NC, LV-sh-CaMK II, and LV-sh-CaMK II-NC). CaMK II: calcium-calmodulin-dependent protein kinase type 2; AIF: apoptosis-inducing factor; LV: lentivirus; NC: negative control; sh: short hairpin RNA; (n = 6/group). **B**, The ratio of CaMK II/β-actin in 5 groups. CaMK II: calcium-calmodulin-dependent protein kinase type 2; LV: lentivirus; NC: negative control; sh: short hairpin RNA; (n = 6/group, $^{**}p<0.01$). **C**, The ratio of cytochrome c/β-actin in 5 groups. CaMK II: calcium-calmodulin-dependent protein kinase type 2; LV: lentivirus; NC: negative control; sh: short hairpin RNA; (n = 6/group, $^{**}p<0.01$). **D**, The ratio of AIF/β-actin in 5 groups. AIF: apoptosis-inducing factor; CaMK II: calcium-calmodulin-dependent protein kinase type 2; LV: lentivirus; NC: negative control; sh: short hairpin RNA; (n = 6/group, $^{**}p<0.01$).

Consistent with the cell experiment, WB analysis revealed after overexpressing CaMK II, the expression of cytochrome *c* and AIF was increased significantly. When interfering with the expression of CaMK II, the level of cytochrome *c* and AIF has decreased accordingly (Figure 4A to D, $p<0.01$). Transmission electron microscope observed that mitochondrial membrane integrity was destroyed, and the mitochondrial ridge was disordered in the LV- CaMK II group, compared to the control group (Figure 5E). Detection of mitochondrial membrane potential showed that after the overexpression of CaMK II, the ratio of red/green cell was decreased compared with the control group ($p<0.05$). Contrastingly, the ratio of red/green cell appeared to ascend in the LV-sh CaMK II group significantly (Figure 5F, $p<0.01$). The measurement of the concentration of Ca^{2+} indicated that there was no discrepancy among the 4 groups (Figure 5G). Our results revealed that CaMK II activates cytochrome *c*/AIF pathway, and regulates the apoptosis of hepatocyte through promotion of mitochondrial dysfunction.

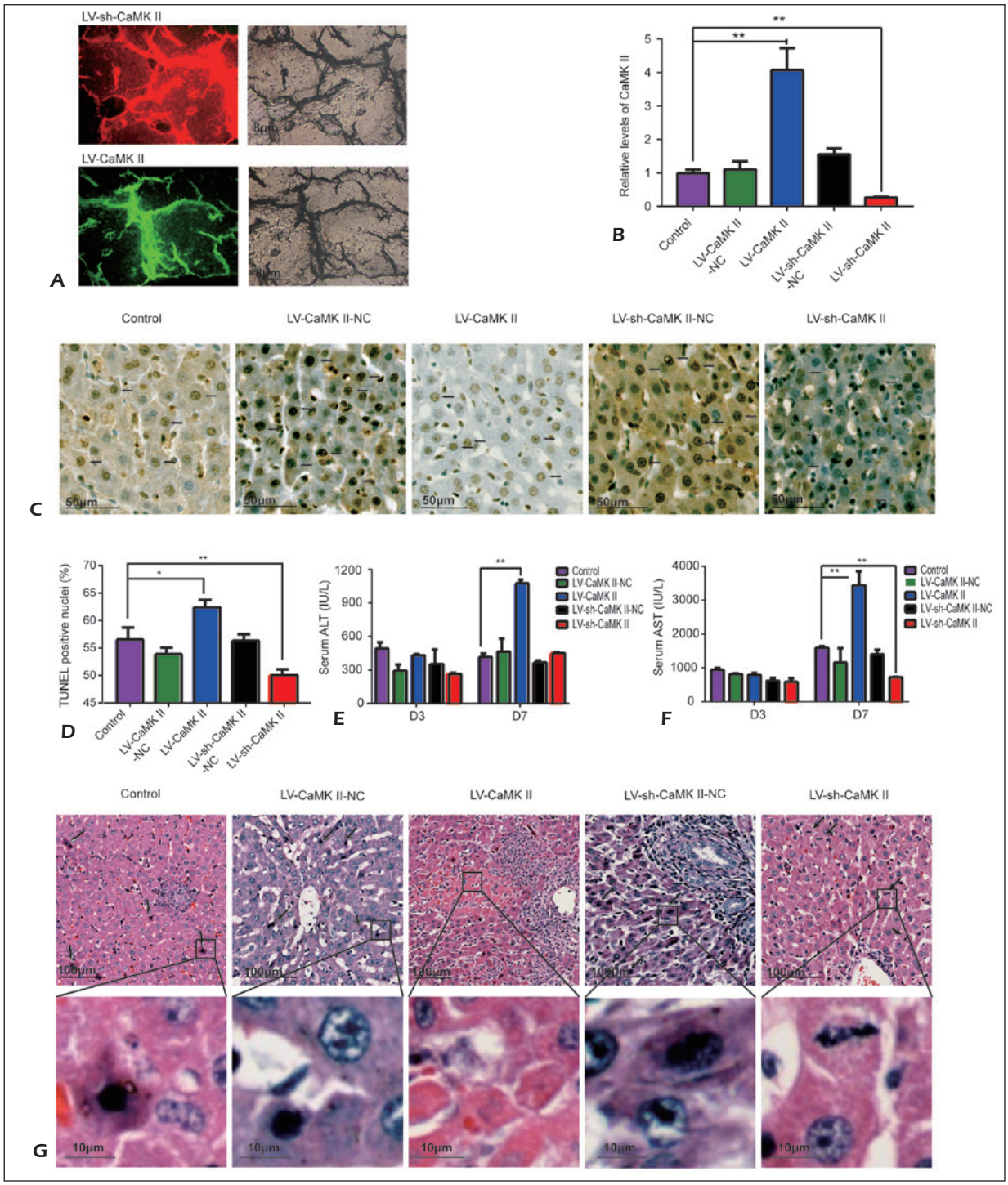

Figure 4. Effect of overexpression and inhibition of CaMK II on apoptosis rate, pathological changes, and liver function. **A**, A fluorescence microscope observed the distribution of viral vectors in the liver. CaMK II: calcium-calmodulin-dependent protein kinase type 2; LV: lentivirus; sh: short hairpin RNA; (n = 6/group, Scale bar = 8 μm). **B**, Relative levels of CaMK II in 5 groups. CaMK II: calcium-calmodulin-dependent protein kinase type 2; LV: lentivirus; NC: negative control; sh: short hairpin RNA; (n = 6/group, $^{**}p<0.01$). **C**, The TUNEL positive cells in the liver tissue in 5 groups. CaMK II: calcium-calmodulin-dependent protein kinase type 2; LV: lentivirus; NC: negative control; sh: short hairpin RNA; (n = 6/group, scale bar = 50 μm). D, The percentage of TUNEL positive nuclei in the liver tissue in 5 groups. CaMK II: calcium-calmodulin-dependent protein kinase type 2; LV: lentivirus; NC: negative control; sh: short hairpin RNA; (n = 6/group, $^{**}p<0.01$). **E**, The serum ALT on D3 and D7 in 5 groups. ALT: alanine aminotransferase; D: day; CaMK II: calcium-calmodulin-dependent protein kinase type 2; LV: lentivirus; NC: negative control; sh: short hairpin RNA. (n = 6/group, $^{*}p<0.05$, $^{**}p<0.01$). **F**, The serum AST on D3 and D7 in 5 groups. AST, aspartate aminotransferase; D: day; CaMK II: calcium-calmodulin-dependent protein kinase type 2; LV: lentivirus; NC: negative control; sh: short hairpin RNA; (n = 6/group, $^{**}p<0.01$). **G**, Pathological observation of liver tissue in 5 groups. CaMK II: calcium-calmodulin-dependent protein kinase type 2; LV: lentivirus; NC: negative control; sh: short hairpin RNA; (n = 6/group, scale bar = 100 μm).

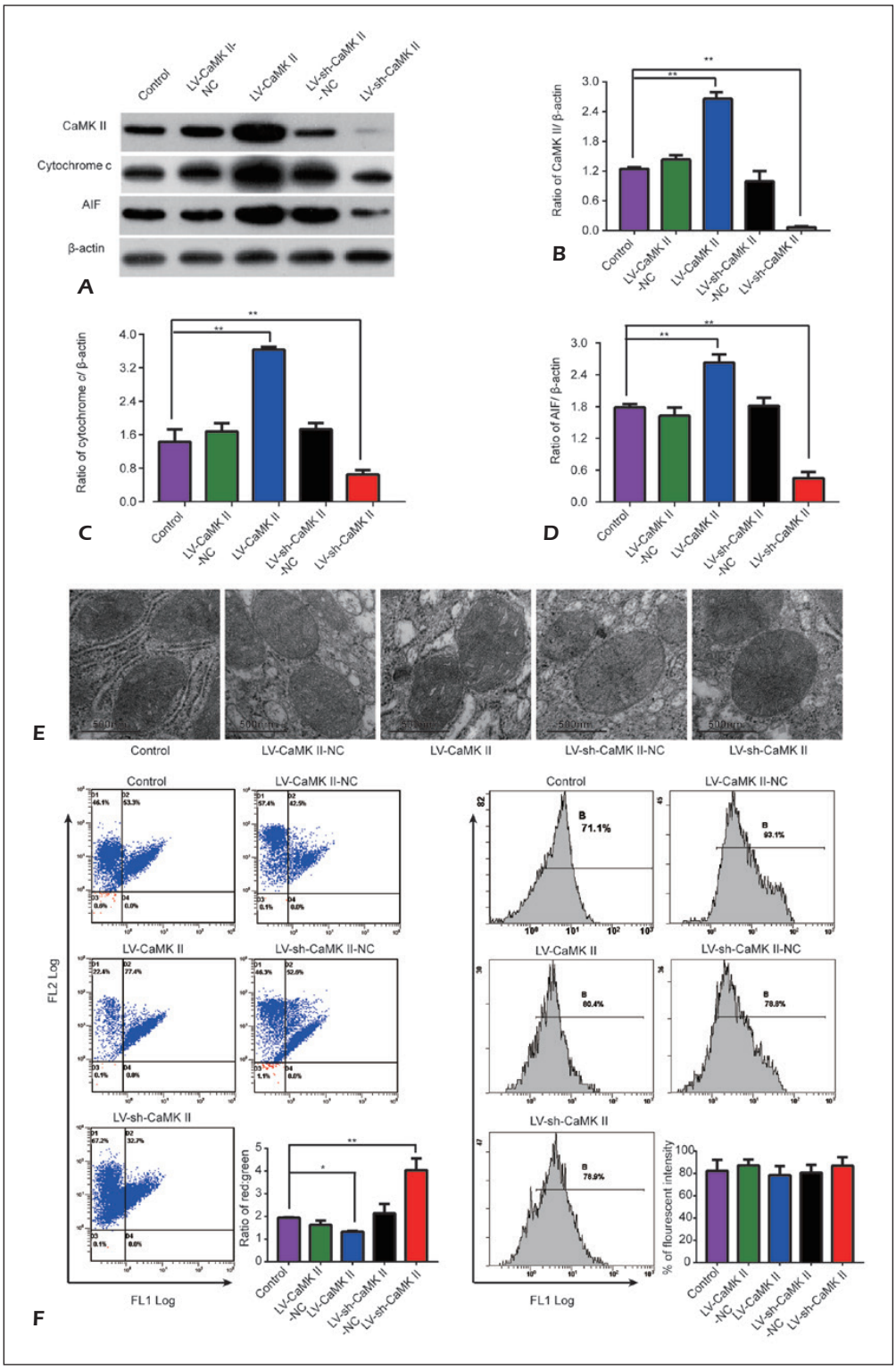

Figure 5. The Study of the CaMK II mechanism regulating apoptosis of hepatocytes. **A**, The protein bands of CaMK II, cytochrome c, and AIF in 5 groups (Control, LV-CaMK II, LV-CaMK II-NC, LV-sh-CaMK II, and LV-sh-CaMK II-NC). CaMK II: calcium-calmodulin-dependent protein kinase type 2; AIF: apoptosis-inducing factor; LV: lentivirus; NC: negative control; sh: short hairpin RNA; (n = 6/group). **B**, The ratio of CaMK II/β-actin in 5 groups. CaMK II: calcium-calmodulin-dependent protein kinase type 2; LV: lentivirus; NC: negative control; sh: short hairpin RNA; (n = 6/group, $^{**}p<0.01$). **C**, The ratio of cytochrome c/β-actin in 5 groups. CaMK II: calcium-calmodulin-dependent protein kinase type 2; LV: lentivirus; NC: negative control; sh: short hairpin RNA; (n = 6/group, $^{**}p<0.01$). **D**, The ratio of AIF/β-actin in 5 groups. AIF: apoptosis-inducing factor; CaMK II: calcium-calmodulin-dependent protein kinase type 2; LV: lentivirus; NC: negative control; sh: short hairpin RNA; (n = 6/group, $^{**}p<0.01$). **E**, Pathological changes of mitochondria in 5 groups. CaMK II: calcium-calmodulin-dependent protein kinase type 2; LV: lentivirus; NC: negative control; sh: short hairpin RNA; (n = 6/group, scale bar = 500 nm). **F**, The ratio of red: green of 5 groups. CaMK II: calcium-calmodulin-dependent protein kinase type 2; LV: lentivirus; NC: negative control; sh: short hairpin RNA; (n = 6/group, $^{*}p<0.05$, $^{**}p<0.01$). **G**, Measurement of the concentration of Ca2+ in intracellular in 5 groups. CaMK II: calcium-calmodulin-dependent protein kinase type 2; LV: lentivirus; NC: negative control; sh: short hairpin RNA; (n = 6/group).

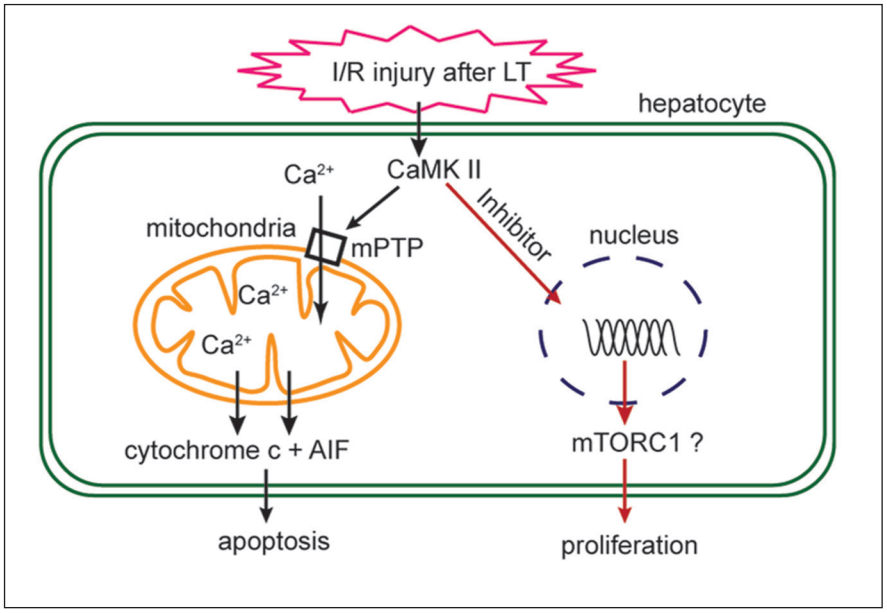

Figure 6. Mechanism of CaMK II regulating hepatocyte apoptosis after I/R injury. I/R injury: ischemia reperfusion injury; LT: liver transplantation; CaMK II: calcium-calmodulin-dependent protein kinase type 2; AIF: apoptosis-inducing factor.

Discussion

In this study, we showed that CaMK II significantly increased after I/R injury, which cause mitochondrial dysfunction and pro-apoptotic factor release. Due to this, liver cells apoptosis occurs. The present research suggests that CaMK II might play a key role in I/R injury after LT, and cytochrome *c*, AIF might be its direct target factor, which provides a new direction for fundamental research and clinical therapeutic strategies.

We found the damage of liver tissues is closely related to the release of CaMK II. These findings reflected 3 aspects: (a) the expression of CaMK II is correlated with WIT. (b) CaMK II is persistently increasing after LT, and the peak can be postponed to D7. (c) The liver pathological changes are closely related to the overexpression of CaMK II. Existing studies have reported that the activation of CaMK II can be triggered on the condition of the ER stress, hyperglycemia, and oxidative stress[25-27], and that CaMK II can increase in early time after I/R injury in cardiomyocytes[14,28]. This is the first investigation to link the expression of CaMK II with the I/R injury in DCD liver. Our findings indicated that the expression of CaMK II appeared to slowly grow, which may explain why the sustained damage of liver tissue is related to the expression of CaMK II.

Previous researches showed that Ca^{2+} can increase in the early stage of I/R injury[29]. The cause of Ca^{2+} release is correlated with the ER stress[20,30], the outcome of ER stress is aberrant Ca^{2+} release[31,32]. Ca^{2+} participates in phospholipase, calpain activation and other functions[33], it can regulate the activation of CaMK II. In turn, the phospholipase of CaMK II can regulate the influx of Ca^{2+} into the mitochondria[18]. Once the Ca^{2+} overloads in the mitochondria, the mitochondria respond to the change of mitochondrial permeability, and the proapoptotic factors were released[34], then the hepatocyte initiates cell apoptosis.

CaMK II is a multifunction regulator protein, which plays a key role in the intercellular junction and the pathological process, including inducing the I/R injury in special tissue. There is enough evidence that CaMK II and mitochondrial apoptosis can increase after I/R injury[14,28]. Joiner et al[23] found that CaMK II activity can regulate the Ca^{2+} influx in mitochondria and accelerate cell apoptosis. Li et al[35] reported that CaMK II activity can lead to the impairment of astrocytes in ischemia neuron death. However, the mechanism of CaMK II functions as I/R injury in LT is still unknown. Our results over the I/R injury of DCD liver are listed on the model in Figure 6. The current study suggests that the expression of CaMK II promotes the apoptosis of hepatocyte[21]. Further research indicated that prolonged warm ischemia time increases the expression of CaMK II, which will lead to the overload of Ca^{2+} in the hepatocyte; a

report showed that the intracellular Ca^{2+} increasing is correlated with the ER stress when the cell undergoes ROS and damage. The intracellular Ca^{2+} influx accumulation is regulated by the CaMK II[20]. Ca^{2+} overload will lead to mitochondrial permeability transition, which will cause the mitochondrial permeability. Those changes result in the release of proapoptotic factors in the mitochondria, such as cytochrome *c* and AIF. It has been observed that cytochrome *c* and AIF can activate caspase 3, which is the important factor for cell apoptosis[36,37]. Finally, mitochondrial apoptosis will be initiated, and cause the hepatocyte death. After inhibiting the expression of CaMK II, the mitochondrial apoptosis pathway will be suppressed. Therefore, the I/R injury will be alleviated. Therefore, inhibiting the expression of CaMK II can be utilized in the I/R injury treatment after LT. Another finding shows that, after decreasing the expression of CaMK II, the hepatocytes appeared to proliferate, which was reflected in our *in vitro* and *in vivo* experiment. *In vitro*, hepatocytes either appeared to reduce cell apoptosis or improve cell activity, and the cell cycle of the S phase started to extend. *In vivo* experiment, we can recognize the division stage of hepatocytes in the liver tissue. Our ongoing research managed to explain the proliferation phenomenon. Results regarding hepatocarcinogenesis established that the deletion of CaMK II can enhance the activation of mTORC1 and promote the hyperproliferation of hepatocytes. However, the mechanism of CaMK II function as the hepatocytes suffering from I/R injury need further studies[38].

Conclusions

We discovered that CaMK II is a promotor which accelerates the damage of I/R injury undergoing prolonged WIT. The benefit of suppression of the expression of CaMK II in the DCD liver depends on: (a) decreasing the hepatocyte apoptosis and alleviating the liver damage after LT; (b) promoting the hepatocyte proliferation and recovering from the warm ischemia injury.

Acknowledgements

The authors thank Dr. Jiang-Hua Ran (Department of Hepatobiliary Pancreas and Vascular, Kunming Municipal First People's Hospital, Kunming, Yunnan, China) for the critical comment and discussion on this study. This research was supported by the National Natural Science Foundation of China under the grant [Grant No. NSF 81660112]; and the Yunnan Provincial Science and Technology Department-Kunming Medical University under the grant [Grant No. 2015FA010].

Conflict of Interests

The authors declare that they have no conflict of interests.

References

1) Mihaylov P, Mangus R, Ekser B, Cabrales A, Timsina L, Fridell J, Lacerda M, Ghabril M, Nephew L, Chalasani N, Kubal CA. Expanding the donor pool with utilization of extended criteria DCD livers. Liver Transpl 2019; 25: 1198-1208.
2) Pitarch Martinez M, Sanchez Perez B, Leon Diaz FJ, Fernandez Aguilar JL, Perez Daga JA, Montiel Casado MC, Aranda Narváez JM, Suárez Muñoz MÁ, Santoyo Santoyo J. Donation after cardiac death in liver transplantation: an additional source of organs with similar results to donation after brain death. Transplant Proc 2019; 51: 4-8.
3) Jadlowiec CC, Taner T. Liver transplantation: current status and challenges. World J Gastroenterol 2016; 22: 4438-4445.
4) Smith M, Dominguez-Gil B, Greer DM, Manara AR, Souter MJ. Organ donation after circulatory death: current status and future potential. Intensive Care Med 2019; 45: 310-321.
5) Mazaheri M, Mojtabaee M, Mohsenzadeh M, Shahryari S, Sadegh Beigee F. Liver donation from marginal donors: to donate or not to donate? Exp Clin Transplant 2019; 17 (Suppl 1): 254-256.
6) Doyle MB, Collins K, Vachharajani N, Lowell JA, Shenoy S, Nalbantoglu I, Byrnes K, Garonzik-Wang J, Wellen J, Lin Y, Chapman WC. Outcomes using grafts from donors after cardiac death. J Am Coll Surg 2015; 221: 142-152.
7) Olthof PB, van Golen RF, Meijer B, van Beek AA, Bennink RJ, Verheij J, van Gulik TM, Heger M. Warm ischemia time-dependent variation in liver damage, inflammation, and function in hepatic ischemia/reperfusion injury. Biochim Biophys Acta Mol Basis Dis 2017; 1863: 375-385.
8) Go KL, Lee S, Zendejas I, Behrns KE, Kim JS. Mitochondrial dysfunction and autophagy in hepatic ischemia/reperfusion injury. Biomed Res Int 2015; 2015: 183469.
9) Morrissey PE, Monaco AP. Donation after circulatory death: current practices, ongoing challenges, and potential improvements. Transplantation 2014; 97: 258-264.
10) Coffey JC, Wanis KN, Monbaliu D, Gilbo N, Selzner M, Vachharajani N, Levstik MA, Marquez M, Doyle MBM, Pirenne J, Grant D, Heimbach JK, Chapman W, Vogt K, Hernandez-Alejandro R. The influence of functional warm ischemia time on DCD liver transplant recipients' outcomes. Clin Transplant 2017; 31. doi: 10.1111/ctr.13068

11) Liu S, Miao J, Shi X, Wu Y, Jiang C, Zhu X, Wu X, Ding Y, Xu Q. Risk factors for post-transplant death in donation after circulatory death liver transplantation. J Invest Surg 2018; 31: 393-401.
12) Le Dinh H, de Roover A, Kaba A, Lauwick S, Joris J, Delwaide J, Honoré P, Meurisse M, Detry O. Donation after cardio-circulatory death liver transplantation. World J Gastroenterol 2012; 18: 4491-4506.
13) Nieuwenhuijs VB, De Bruijn MT, Padbury RT, Barritt GJ. Hepatic ischemia-reperfusion injury: roles of Ca2+ and other intracellular mediators of impaired bile flow and hepatocyte damage. Dig Dis Sci 2006; 51: 1087-1102.
14) Sun CK, Zhang XY, Sheard PW, Mabuchi A, Wheatley AM. Change in mitochondrial membrane potential is the key mechanism in early warm hepatic ischemia-reperfusion injury. Microvasc Res 2005; 70: 102-110.
15) Leistner M, Sommer S, Kanofsky P, Leyh R, Sommer SP. Ischemia time impacts on respiratory chain functions and Ca(2+)-handling of cardiac subsarcolemmal mitochondria subjected to ischemia reperfusion injury. J Cardiothorac Surg 2019; 14: 92.
16) Wyss RK, Mendez-Carmona N, Sanz MN, Arnold M, Segiser A, Fiedler G M, Carrel TP, Djafarzadeh S, Tevaearai Stahel HT, Longnus SL. Mitochondrial integrity during early reperfusion in an isolated rat heart model of donation after circulatory death-consequences of ischemic duration. J Heart Lung Transplant 2019; 38: 647-657.
17) Kim JS, He L, Qian T, Lemasters JJ. Role of the mitochondrial permeability transition in apoptotic and necrotic death after ischemia/reperfusion injury to hepatocytes. Curr Mol Med 2003; 3: 527-535.
18) Swulius MT, Waxham MN. Ca(2+)/calmodulin-dependent protein kinases. Cell Mol Life Sci 2008; 65: 2637-2657.
19) Simon B, Huart AS, Wilmanns M. Molecular mechanisms of protein kinase regulation by calcium/calmodulin. Bioorg Med Chem 2015; 23: 2749-2760.
20) Timmins JM, Ozcan L, Seimon TA, Li G, Malagelada C, Backs J, Backs T, Bassel-Duby R, Olson EN, Anderson ME, Tabas I. Calcium/calmodulin-dependent protein kinase II links ER stress with Fas and mitochondrial apoptosis pathways. J Clin Invest 2009; 119: 2925-2941.
21) Salas MA, Valverde CA, Sanchez G, Said M, Rodriguez JS, Portiansky EL, Kaetzel MA, Dedman JR, Donoso P, Kranias EG, Mattiazzi A. The signalling pathway of CaMKII-mediated apoptosis and necrosis in the ischemia/reperfusion injury. J Mol Cell Cardiol 2010; 48: 1298-1306.
22) Federico M, Portiansky EL, Sommese L, Alvarado FJ, Blanco PG, Zanuzzi CN, Dedman J, Kaetzel M, Wehrens XHT, Mattiazzi A, Palomeque J. Calcium-calmodulin-dependent protein kinase mediates the intracellular signalling pathways of cardiac apoptosis in mice with impaired glucose tolerance. J Physiol 2017; 595: 4089-4108.
23) Joiner MLA, Koval OM, Li J, He BJ, Allamargot C, Gao Z, Luczak ED, Hall DD, Fink BD, Chen B, Yang J, Moore SA, Scholz TD, Strack S, Mohler PJ, Sivitz WI, Song LS, Anderson ME. CaMKII determines mitochondrial stress responses in heart. Nature 2012; 491: 269-273.
24) Oldani G, Lacotte S, Morel P, Mentha G, Toso C. Orthotopic liver transplantation in rats. J Vis Exp 2012.
25) Li J, Wang P, Yu S, Zheng Z, Xu X. Calcium entry mediates hyperglycemia-induced apoptosis through Ca(2+)/calmodulin-dependent kinase II in retinal capillary endothelial cells. Mol Vis 2012; 18: 2371.
26) Bracken C, Beauverger P, Duclos O, Russo RJ, Rogers KA, Husson H, Natoli TA, Ledbetter SR, Janiak P, Ibraghimov-Beskrovnaya O, Bukanov NO. CaMKII as a pathological mediator of ER stress, oxidative stress, and mitochondrial dysfunction in a murine model of nephronophthisis. Am J Physiol Renal Physiol 2016; 310: F1414-1422.
27) Toledo FD, Perez LM, Basiglio CL, Ochoa JE, Sanchez Pozzi EJ, Roma MG. The Ca(2)(+)-calmodulin-Ca(2)(+)/calmodulin-dependent protein kinase II signaling pathway is involved in oxidative stress-induced mitochondrial permeability transition and apoptosis in isolated rat hepatocytes. Arch Toxicol 2014; 88: 1695-1709.
28) Uemura A, Naito Y, Matsubara T. Dynamics of ja:math /calmodulin-dependent protein kinase II following acute myocardial ischemia—translocation and autophosphorylation. Biochem Biophys Res Commun 2002; 297: 997-1002.
29) Duvigneau JC, Kozlov AV, Zifko C, Postl A, Hartl RT, Miller I, Gille L, Staniek K, Moldzio R, Gregor W, Haindl S, Behling T, Redl H, Bahrami S. Reperfusion does not induce oxidative stress but sustained endoplasmic reticulum stress in livers of rats subjected to traumatic-hemorrhagic shock. Shock 2010; 33: 289-298.
30) Dara L, Ji C, Kaplowitz N. The contribution of endoplasmic reticulum stress to liver diseases. Hepatology 2011; 53: 1752-1763.
31) Pallet N, Fougeray S, Beaune P, Legendre C, Thervet E, Anglicheau D. Endoplasmic reticulum stress: an unrecognized actor in solid organ transplantation. Transplantation 2009; 88: 605-613.
32) Doroudgar S, Thuerauf DJ, Marcinko MC, Belmont PJ, Glembotski CC. Ischemia activates the ATF6 branch of the endoplasmic reticulum stress response. J Biol Chem 2009; 284: 29735-29745.
33) Pittas K, Vrachatis DA, Angelidis C, Tsoucala S, Giannopoulos G, Deftereos S. The role of calcium handling mechanisms in reperfusion injury. Curr Pharm Des 2018; 24: 4077-4089.
34) Hurst S, Hoek J, Sheu SS. Mitochondrial Ca(2+) and regulation of the permeability transition pore. J Bioenerg Biomembr 2017; 49: 27-47.
35) Liu Z, Huang Y, Liu L, Zhang L. Inhibitions of PKC and CaMK-II synergistically rescue ischemia-induced astrocytic dysfunction. Neurosci Lett 2017; 657: 199-203.
36) Jiang X, Wang X. Cytochrome C-mediated apoptosis. Annu Rev Biochem 2004; 73: 87-106.
37) Nikoletopoulou V, Markaki M, Palikaras K, Tavernarakis N. Crosstalk between apoptosis, necrosis and autophagy. Biochim Biophys Acta 2013; 1833: 3448-3459.
38) Meng Z, Ma X, Du J, Wang X, He M, Gu Y, Zhang J, Han W, Fang Z, Gan X, Van Ness C, Fu X, Schones DE, Xu R, Huang W. CAMK2gamma antagonizes mTORC1 activation during hepatocarcinogenesis. Oncogene 2017; 36: 2446-2456.